LAMINAR BOUNDARY LAYER ON THE WALLS OF AN AXISYMMETRIC CHANNEL IN THE PRESENCE OF SWIRLS IN THE EXTERNAL STREAM

V. V. Bogdanova

UDC 532.526.2

The numerical solution of the problem of laminar, viscous, incompressible fluid flow in the boundary layer on the walls of an axisymmetric channel is considered for the presence of swirls in the external stream. The fundamental boundary-layer characteristics are obtained for several channels.

1. Formation of the Problem

Let us consider the laminar motion of a viscous incompressible fluid in the boundary layer on the walls of an axisymmetric channel with curvilinear generatrix. In this case the boundary layer equations have the following form [1]:

$$u\frac{\partial u}{\partial x}+v\frac{\partial u}{\partial y}-\frac{w^2r'}{r}=UU'-\frac{W^2r'}{r}+\nu\frac{\partial^2 u}{\partial y^2}, \tag{1}$$

$$u\frac{\partial w}{\partial x}+v\frac{\partial w}{\partial y}+\frac{uwr'}{r}=\nu\frac{\partial^2 w}{\partial y^2}, \tag{2}$$

$$\frac{\partial(ru)}{\partial x}+\frac{\partial(rv)}{\partial y}=0. \tag{3}$$

The boundary conditions are $u = v = w = 0$ for $y = 0$, and $u \to U(x)$, $w \to W(x)$ for $y \to \infty$. Here $r(x)$ is the radius of the channel section, the x axis is directed along the channel generatrix while y is perpendicular to the channel wall; u and v, velocity components in the boundary layer along the x and y axes, respectively; w, circumferential velocity component in the boundary layer; U and W, longitudinal and circumferential velocity components in the external stream; ν, coefficient of kinematic viscosity; and the prime signifies differentiation with respect to x.

Let us introduce the new variable

$$\eta=y\sqrt{\frac{U}{2\nu x}}.$$

We shall seek the longitudinal and circumferential velocity components in the boundary layer in the form

$$u=U\frac{\partial\Phi(\eta,\ x)}{\partial\eta},\quad w=W\varphi(\eta,\ x).$$

There then follows from the incompressiblity equation

$$v=-\sqrt{2\nu xU}\left[\Phi\left(\frac{r'}{r}+\frac{1}{2x}+\frac{1}{2}\frac{U'}{U}\right)+\frac{\partial\Phi}{\partial\eta}\frac{\partial\eta}{\partial x}+\frac{\partial\Phi}{\partial x}\right].$$

Substituting the expressions for u, v, and w into (1) and (2), we obtain

$$\begin{aligned}&\frac{\partial^3\Phi}{\partial\eta^3}+\left(1+2x\frac{r'}{r}+x\frac{U'}{U}\right)\Phi\frac{\partial^2\Phi}{\partial\eta^2}+2x\frac{U'}{U}\left[1-\left(\frac{\partial\Phi}{\partial\eta}\right)^2\right]-\\&-\frac{W^2}{U^2}\frac{r'}{r}2x(1-\varphi^2)=2x\left(\frac{\partial\Phi}{\partial\eta}\frac{\partial^2\Phi}{\partial\eta\partial x}-\frac{\partial\Phi}{\partial x}\frac{\partial^2\Phi}{\partial\eta^2}\right),\\&\frac{\partial^2\varphi}{\partial\eta^2}+\left(1+2x\frac{r'}{r}+x\frac{U'}{U}\right)\Phi\frac{\partial\varphi}{\partial\eta}=2x\left(\frac{\partial\varphi}{\partial x}\frac{\partial\Phi}{\partial\eta}-\frac{\partial\varphi}{\partial\eta}\frac{\partial\Phi}{\partial x}\right).\end{aligned} \tag{4}$$

M. I. Kalinin Leningrad Polytechnic Institute. Translated from Inzhenerno-Fizicheskii Zhurnal, Vol. 36, No. 5, pp. 861-868, May, 1979. Original article submitted June 12, 1978.

0022-0841/79/3605- 0573$07.50

The boundary conditions are

$$\frac{\partial\Phi}{\partial\eta} = \Phi = \varphi = 0 \text{ for } \eta = 0;$$

$$\frac{\partial\Phi}{\partial\eta} \to 1,\ \varphi \to 1 \text{ for } \eta \to \infty;$$

$$\frac{\partial\Phi}{\partial\eta} = \frac{\partial\Phi_0(\eta)}{\partial\eta},\ \varphi = \varphi_0(\eta) \text{ for } x = x_0. \tag{5}$$

2. Determination of the External Stream Characteristics

The channel shape r(x) and the external stream velocity are considered known when integrating the system of boundary-layer equations (4). The velocity U(x) is defined as the velocity on the channel walls when an ideal fluid flows. The circumferential velocity component W(x) is given as the velocity caused by a potential vortex located on the channel axis.

The channel shape and the velocity U(x) on the walls were computed by using two theoretical methods expounded in [2-4].

The first method [2, 3] permits the determination of the channel shape and the velocity field in the channel by means of a given velocity distribution along the channel axis. The second method [4] solves this same problem for a given velocity profile at the channel entrance.

If the function characterizing the velocitydistribution along the channel axis z is selected in the first method in the form

$$f_0(z) = A + \frac{B}{\sqrt{2\pi}}\int_0^z \exp\left(-\frac{z^2}{2}\right) dz,$$

then the stream function Ψ and the axial V_z and radial V_r velocity components can be written as

$$\Psi(z, r) = B\sum_{n=2}^{\infty} \frac{(-1)^n\, 2nR^n}{(n!)^2} \frac{\exp\left(-\frac{z^2}{2}\right)}{\sqrt{2\pi}} H_{2n-3}(z) + 2Rf_0(z), \tag{6}$$

$$V_z(z, r) = B\sum_{n=1}^{\infty} \frac{(-1)^{n-1} R^n \exp\left(-\frac{z^2}{2}\right)}{(n!)^2\sqrt{2\pi}} H_{2n-1}(z) + f_0(z), \tag{7}$$

$$V_r(z, r) = B\sum_{n=1}^{\infty} \frac{(-1)^n\, nR^{\frac{2n-1}{2}}}{(n!)^2} \frac{\exp\left(-\frac{z^2}{2}\right)}{\sqrt{2\pi}} H_{2n-2}(z), \tag{8}$$

where H_n are Hermite polynomials, $R = r^2/4$, and A and B are constants.

It follows from (7) that for $z \to \mp\infty$ on the channel axis (r = 0), the axial velocity component V_z tends, respectively, to the quantities

$$(V_z)_{-\infty} = A - \frac{1}{2}B \text{ and } (V_t)_{+\infty} = A + \frac{1}{2}B. \tag{9}$$

The channel shape was determined from the solution of the equation

$$B\sum_{n=2}^{\infty} \frac{(-1)^n\, 2nR^n}{(n!)^2} \frac{\exp\left(-\frac{z^2}{2}\right)}{\sqrt{2\pi}} H_{2n-3} + 2Rf_0 = \Psi = \text{const}. \tag{10}$$

For computation it is convenient to write (6)-(8) as

$$V_z = f_0 + \sum_{n=1}^{\infty} a_n,\ V_r = \sum_{n=1}^{\infty} b_n, \tag{11}$$

$$R = \frac{\Psi}{2f_0} + \sum_{n=2}^{\infty} c_n, \tag{12}$$

where

$$a_{n+1} = -a_n \frac{RH_{2n+1}}{(n+1)^2 H_{2n-1}}; \quad a_1 = \frac{B}{\sqrt{2\pi}} Rz \exp\left(-\frac{z^2}{2}\right);$$

$$b_{n+1} = -b_n \frac{RH_{2n}}{n(n+1) H_{2n-2}}. \quad b_1 = -\frac{B}{\sqrt{2\pi}} R^{1/2} \exp\left(-\frac{z^2}{2}\right);$$

$$c_{n+1} = -c_n \frac{RH_{2n-1}}{n(n+1) H_{2n-3}}; \quad c_2 = \frac{B}{\sqrt{2\pi}} R^2 z \frac{\exp\left(-\frac{z^2}{2}\right)}{2f_0}.$$

The velocity distribution at the channel entrance in the second method [4] is given in the form

$$(V_z)_{z=0} = \frac{V_0}{\sqrt{1-(r/c)^2}},$$

where V_0 is the axial velocity at the entrance section; $c = \sqrt{\alpha^2/(\alpha^2-1)}a$; a, radius of the entrance section; and α, ratio between the velocity at the wall and on the axis of the entrance section ($\alpha > 1$).

Then the dimensionless stream function $\bar{\Psi}$ and the axial and radial velocity components are determined by the following formulas:

$$\bar{\Psi} = 2B_1 R + 2A_1 \sum_{n=0}^{\infty} \frac{(-1)^n (2n)!\, R^{n+1} \sin[(2n+1)y]}{n!\,(n+1)!\,(1+\bar{z}^2)^{\frac{2n+1}{2}}}, \tag{13}$$

$$\bar{V}_z = B_1 + A_1 \sum_{n=0}^{\infty} \frac{(-1)^n (2n)!\, R^n \sin[(2n+1)y]}{(n!)^2\,(1+\bar{z}^2)^{\frac{2n+1}{2}}}, \tag{14}$$

$$\bar{V}_r = A_1 \sum_{n=0}^{\infty} \frac{(-1)^n (2n+1)!\, R^{n+1/2} \sin[(2n+2)y]}{n!\,(n+1)!\,(1+\bar{z}^2)^{n+1}}, \tag{15}$$

where $\bar{V}_Z = V_Z/V_0$; $\bar{V}_r = V_r/V_0$; $\bar{\Psi} = \Psi/V_0 c^2$; $\bar{z} = z/c$; $\bar{r} = r/c$; $y = \arctan 1/\bar{z}$; A_1 and B_1 are constants.

Let us rewrite (13)-(15) in a convenient form for computation:

$$R = \frac{\bar{\Psi}}{2B_1} - \sum_{n=0}^{\infty} c_n, \tag{16}$$

$$\bar{V}_z = B_1 + \sum_{n=0}^{\infty} a_n, \quad \bar{V}_r = \sum_{n=0}^{\infty} b_n, \tag{17}$$

where

$$c_{n+1} = -c_n \frac{2(2n+1) R \sin[(2n+3)y]}{(n+2)\sin[(2n+1)y](1+\bar{z}^2)};$$

$$c_0 = \frac{A_1}{B_1} R \frac{\sin y}{(1+\bar{z}^2)^{1/2}};$$

$$a_{n+1} = -a_n \frac{2(2n+1) R \sin[(2n+3)y]}{(n+1)(1+\bar{z}^2)\sin[(2n+1)y]}; \quad a_0 = A_1 \frac{\sin y}{(1+\bar{z}^2)^{1/2}};$$

$$b_{n+1} = -b_n \frac{2(2n+3) R \sin[(2n+4)y]}{(n+2)(1+\bar{z}^2)\sin[(2n+2)y]};$$

$$b_0 = A_1 R^{1/2} \frac{\sin 2y}{1+\bar{z}^2}.$$

The channel shape is determined from (16) in this method, where $\bar{\Psi}$ is assumed constant.

Equations (12) and (16) were solved by successive approximations. The iterations were continued until the ratio $(R^{i+1} - R^i)/R(z)$ exceeded 10^{-5} (i is the number of the iteration). The velocities $V_z(z)$ and $V_r(z)$ on the channel walls were determined by using (11) or (17) by means

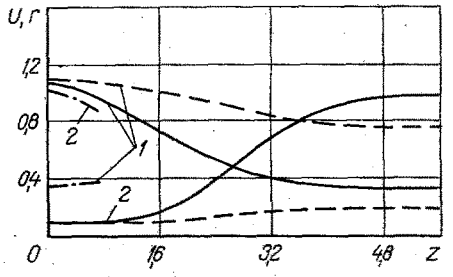

Fig. 1

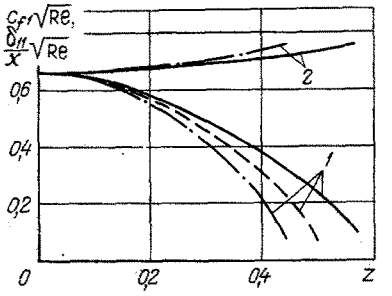

Fig. 2

Fig. 1. Channel shape (1) and change in longitudinal velocity in the external stream along the channel axis (2): solid lines are for the contractor K1 and the diffusor D1, while the dashed line is for contractor K2 and the dash–dot lines are for D2.

Fig. 2. Curves of the change in the friction coefficient $c_{f_1}\sqrt{Re}$ (1) and the dimensionless provisional boundary-layer thickness $(\delta_{11}/x)\sqrt{Re}$ (2) along the diffusor D2 axis for $\Gamma = 0$ (solid lines); $\Gamma = 0.22$ (dashes); $\Gamma = 0.32$ (dash–dot lines).

of the functions R(z) found. Terms on the order of $>10^{-4}$ were retained in all the computational formulas.

One diffusor (D1) and two contractors (K1 and K2) were constructed by using the first method, and one diffusor (D2) by using the second. The following values were taken for the constants: A = 0.55 and B = 0.9 in the computation of the contractor K1 and the diffusor D1; A = 0.15, B = 0.1 for the contractor K2; and $A_1 = 0.3$ and $B_1 = 0.7$ for the diffusor D2. It follows from (9) that a tenfold increase in the velocity occurs in the contractor K1 and a twofold increase in the contractor K2. In all cases $\Psi = 0.06$.

The circumferential and longitudinal velocity components in the external stream were determined by the following formulas:

$$W = \Gamma/r,\ U = \sqrt{V_z^2 + V_r^2},$$

where Γ is a given constant defining the swirl in the external stream.

The shape of the computed channels and the dependence of the external stream velocity U on the coordinate z are represented in Fig. 1.

3. Integration of the Boundary-Layer Equation

System (4) was integrated by a numerical method for the above-mentioned channels for different values of the quantities Γ.

Let us note that (4) goes over into two Blasius equations ($\varphi = \partial\Phi/\partial\eta$) for x = 0. Keeping this in mind and taking into account that all the computed channels are channels with two asymptotes, we take as initial condition for the system (4): for x = 0 $\partial\Psi/\partial\eta = \partial\Phi_0/\partial\eta$, where Φ_0 is the solution of the Blasius equation.

The range of integration in η was bounded by the quantity $\eta_\infty = 7.5$, and the second of the boundary conditions (5) was replaced by the following:

$$\partial\Phi/\partial\eta = 1,\ \varphi = 1 \text{ for } \eta = 7.5.$$

As computations showed, the longitudinal and circumferential velocity profiles approach sufficiently close to 1 for $\eta < 7.5$.

The order of the first equation in system (4) was reduced for the integration by means of the substitution

$$\omega = \partial\Phi/\partial\eta$$

The derivatives with respect to x in (4) were replaced by difference analogs by a two-point scheme. Consequently, a system of two nonlinear second-order differential equations was obtained which was integrated at each x spacing by using the method of factorization with iterations. This system had the following form in x at the i-th layer in the n-th approximation:

$$\frac{\partial^2\omega}{\partial\eta^2}+\frac{\partial\omega}{\partial\eta}\left(L_1\Phi_{n-1}+2x\,\frac{\Phi_{n-1}-\Phi_{i-1}}{h}\right)-\omega\omega_{n-1}\left(L_2+\frac{2x}{h}\right)+L_2-L_3(1-\varphi_{n-1}^2)+2x\,\frac{\omega_{n-1}\omega_{i-1}}{h}=0,\tag{18}$$

$$\frac{\partial^2\varphi}{\partial\eta^2}+\frac{\partial\varphi}{\partial\eta}\left(L_1\Phi_{n-1}+2x\,\frac{\Phi_{n-1}-\Phi_{i-1}}{h}\right)-\varphi\,2x\,\frac{\omega_{n-1}}{h}+2x\,\frac{\omega_{n-1}\varphi_{i-1}}{h}=0,$$

where the following notation was introduced:

$$\Phi=\int_0^\eta\omega d\eta;\ L_1=2x\,\frac{r'}{r}+1+x\,\frac{U'}{U};\ L_2=2x\,\frac{U'}{U};\ L_3=2x\,\frac{W^2}{U^2}\,\frac{r'}{r};$$

h is the spacing in the variable x.

The spacing in the variable η was 0.05 and in the variable x was 0.01.

The characteristic boundary-layer quantities were calculated by means of the longitudinal and circumferential velocity profiles determined as a result of integration of system (18):

the friction coefficient in the longitudinal direction

$$c_{f1}=\frac{\mu\left(\frac{\partial u}{\partial y}\right)_{y=0}}{\rho U^2/2};$$

the friction coefficient in the circumferential direction

$$c_{f2}=\frac{\mu\left(\frac{\partial w}{\partial y}\right)_{y=0}}{\rho UW/2};$$

the provisional boundary-layer thicknesses

$$\delta_n=\int_0^\infty\left(1-\frac{u_n}{U_n}\right)dy;$$

$$\delta_{mn}=\int_0^\infty\frac{u_m}{U_m}\left(1-\frac{u_n}{U_n}\right)dy\,(n=1,\ 2;\ m=1,\ 2);$$

where the subscript 1 corresponds to the longitudinal, and the subscript 2 to the circumferential velocity.

These characteristics were computed by means of the following formulas:

$$c_{f1}\sqrt{\mathrm{Re}}=\sqrt{2}\left(\frac{\partial^2\Phi}{\partial\eta^2}\right)_{\eta=0},\ c_{f2}\sqrt{\mathrm{Re}}=\sqrt{2}\left(\frac{\partial\varphi}{\partial\eta}\right)_{\eta=0},$$

$$\frac{\delta_{11}}{x}\sqrt{\mathrm{Re}}=\sqrt{2}\int_0^\infty\frac{\partial\Phi}{\partial\eta}\left(1-\frac{\partial\Phi}{\partial\eta}\right)d\eta,$$

$$\frac{\delta_{12}}{x}\sqrt{\mathrm{Re}}=\sqrt{2}\int_0^\infty\frac{\partial\Phi}{\partial\eta}(1-\varphi)\,d\eta,$$

$$\frac{\delta_{22}}{x}\sqrt{\mathrm{Re}}=\sqrt{2}\int_0^\infty\varphi(1-\varphi)\,d\eta,$$

$$\frac{\delta_1}{x}\sqrt{\mathrm{Re}}=\sqrt{2}\int_0^\infty\left(1-\frac{\partial\Phi}{\partial\eta}\right)d\eta,\ \frac{\delta_2}{x}\sqrt{\mathrm{Re}}=\sqrt{2}\int_0^\infty(1-\varphi)\,d\eta,$$

where $\mathrm{Re}=xU/\nu$.

Certain results of computing the fundamental boundary-layer characteristics are represented in Figs. 2-4.

Curves of the dependences of the friction coefficients in the longitudinal direction $c_{f_1}\sqrt{\mathrm{Re}}$ and one of the provisional boundary-layer thicknesses $(\delta_{11}/x)\sqrt{\mathrm{Re}}$ on z are constructed for the diffusor D2 in Fig. 2. The dependences mentioned are represented for three values of the quantity Γ characterizing the stream swirl Γ = 0, 0.22, 0.32. It is seen from the figure that the separation in the diffusor is shifted upstream as the swirl increases.

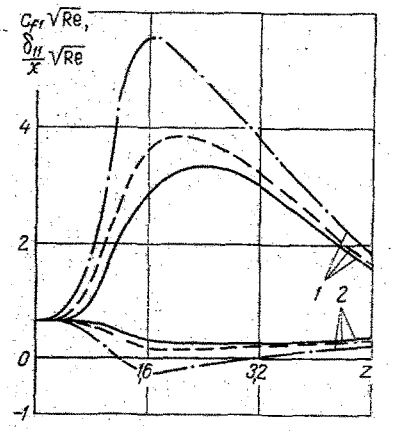

Fig. 3

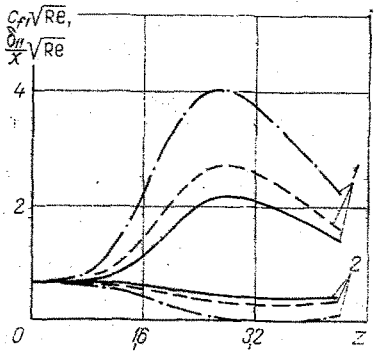

Fig. 4

Fig. 3. Curves of the change in the friction coefficient $c_{f_1}\sqrt{Re}$ (1) and the dimensionless provisional boundary-layer thickness $(\delta_{11}/x)\sqrt{Re}$ (2) along the contractor K1 axis for $\Gamma = 0$ (solid lines); $\Gamma = 0.248$ (dashes); $\Gamma = 0.372$ (dash–dot lines).

Fig. 4. Curves of the change in the friction coefficient $c_{f_1}\sqrt{Re}$ (1) and the dimensionless provisional boundary-layer thickness $(\delta_{11}/x)\sqrt{Re}$ (2) along the contractor K2 axis for $\Gamma = 0$ (solid lines); $\Gamma = 0.248$ (dashes); $\Gamma = 0.372$ (dash–dot).

Analogous curves are placed in Figs. 3 and 4, respectively, for $\Gamma = 0$, 0.248, and 0.372 for the contractors K1 and K2. The friction coefficient $c_{f_1}\sqrt{Re}$ has a maximum at the inflection point of the functions r(z) and U(z) which govern the channel shape and the longitudinal velocity distribution in the external stream (Fig. 1) in both contractors in the absence of a swirl. As a swirl increases, the friction coefficient increases, and the maximum is shifted upstream. The quantity $(\delta_{11}/x)\sqrt{Re}$ has a minimum at these same points. As the swirl increases, $(\delta_{11}/x)\sqrt{Re}$ diminishes and the quantity δ_{11} becomes negative for sufficiently large values. This is explained by the fact that as the swirl increases in contractors, longitudinal velocities exceeding the external stream velocity appear in the boundary layer.

NOTATION

x, axis along the channel generatrix; y, axis perpendicular to the channel wall; u and v, velocity components along the x and y axes in the boundary layer; w, circumferential velocity component in the boundary layer; U and W, longitudinal and circumferential velocity components in the external stream; ν, coefficient of kinematic viscosity; r, radius of the channel section; z, axis along the channel axis; $f_0(z)$, function characterizing the velocity along the channel axis; Ψ, stream function; V_z and V_r, axial and radial velocity components in the channel; H_n, Hermite polynomials; A, B, A_1, B_1, Γ, given constants; V_0, axial velocity in the channel entrance section; a, entrance section radius; c_{f_1} and c_{f_2}, friction coefficients; δ_{11}, δ_{12}, δ_{22}, δ_1, δ_2, provisional boundary-layer thicknesses; Re, Reynolds number; μ, dynamic viscosity coefficient.

LITERATURE CITED

1. V. V. Bogdanova, Proceedings of the Leningrad Polytechnic Institute, Technical Hydrogasdynamics, No. 248 (1965).
2. B. Szczeniowski, J. Aero. Sci., October (1943).
3. H. S. Tsien, J. Aero. Sci., 10, No. 2 (1943).
4. V. G. Sanoyan, Izv. Akad. Nauk Arm. SSR, 9, No. 7 (1956).